Quantitative Investigation of Solitary Pulmonary Nodules with Dynamic Contrast-Enhanced Functional CT

Minming Zhang
Hua Zhou
Yu Zou

Department of Radiology, the First Affiliated Hospital, College of Medicine, Zhejiang University, Hangzhou 310003, China.

Correspondence to: Minming Zhang
Tel: 86-0571-87236509
Fax: 86-0571-87236677
E-mail:zhangminming@163.com

This work was supported by the National Natural Science Foundation of China (No. 30170284).

OBJECTIVE To evaluate solitary pulmonary nodules (SPNs) using quantitative -dynamic contrast -enhancedfunctional -computed tomography (CT); and to illustrate its clinical efficacy in differential diagnosis of benign and malignant pulmonary nodules.

METHODS Eighty patients with non-calcified SPNs (diameter, 5-30 mm) were studied with dynamic contrast-enhanced CT. Patterns of the time-density curves (TDC) were assessed. The precontrast density, peak height in density (PH: the maximum value of the TDC) and S/A ratio (the ratio of the PH of SPN to aorta) were recorded. Precontrast density and enhancement patterns of SPNs were also recorded. Perfusion of the SPNs was calculated.

RESULTS Malignant, benign and inflammatory nodules showed quite different patterns in the TDC. The PH and S/A ratios of the malignant and inflammatory nodules were significantly higher than that of the benign nodules ($P<0.001$; $P<0.001$), while no statistical difference of either the PH or S/A ratio was found between the malignant and inflammatory nodules. Precontrast density of the inflammatory nodules was lower than that of the malignant nodules ($P<0.05$). Both the malignant and inflammatory nodules showed significantly higher perfusions than that of the benign nodules ($P<0.01$; $P<0.01$). However, the difference between the perfusion of the malignant nodules and inflammatory nodules was not significant.

CONCLUSION Dynamic contrast-enhanced functional CT can provide quantitative information regarding blood flow patterns of SPNs and proved to be an alternate non-invasive option in the evaluation and management of solitary pulmonary nodules.

KEYWORKS: solitary pulmonary nodules, computed tomography, contrast-enhanced, dynamic CT.

A solitary pulmonary nodule (SPN) on a chest radiograph represents a major diagnostic dilemma. In clinical practice, the goals of management are to resect malignant tumors without delay and to avoid unnecessary thoracotomy if the nodule is benign. So, the ultimate goal of imaging in the evaluation of SPNs is to accurately distinguish benign from potentially malignant lesions. However, these goals cannot be met in all cases, owing to the difficulty distinguishing benign from malignant nodules, even with advances in imaging

Received June 8, 2004; accepted August 25, 2004.

techniques.

Because of the process of angiogenesis in malignant tumors, the blood supplies of malignant nodules are qualitatively and quantitatively different from that of the most benign nodules. [1,2] These differences may offer an opportunity to distinguish benign from malignant lung nodules by using radiologic imaging technology. Based on the density changes in tissues after injection of contrast media, dynamic CT is able to estimate the pharmacokinetics of contrast media in the organ or tissue. [3-5] Dynamic CT has recently emerged as a promising method for evaluation of renal function, hepatic cirrhosis, occult metastasis, and pulmonary tumors. [6-11] In the present study, dynamic CT was undertaken to describe the blood flow patterns of SPNs combined with pathologic analyses. The purpose of our study was to evaluate SPNs using quantitative-functional analysis with dynamic contrast-enhanced CT and to illustrate its clinical efficacy in differential diagnosis of benign and malignant pulmonary nodules.

MATERIALS AND METHODS

Patients were selected on the basis of the presence of SPN with no calcification and which were smaller than 30 mm in diameter, the absence of contraindications to the administration of contrast medium, and the probable ability to cooperate with the procedure.

Before the examination began, patients were carefully instructed in the breath-holding technique followed by practice in order to reproduce precisely the same degree of inspiration or expiration for each scan series. In addition, and they were given oxygen inspiration at 4 L^3/min. Scans were obtained after breath holding either during inspiration or expiration.

Before the dynamic scan, control scans were obtained from which the best scan level demonstrating the nodule was selected. Single-location dynamic scans were performed at the selected section on a HiSpeed Advantage RP scanner (GE medical systems). Iodinated, low-osmolar, non-ionic contrast medium (Iopamidol 300 or Iohexol 300) was administered via the antecubital vein using an autoinjector at the rate of 4 ml/sec for a total of 100 ml. The section thickness was 5-mm and scanning time was 1 s. Two series of dynamic CT scan sequences were obtained beginning at 15 s (early phase), 75 s (late phase) after the injection. Twenty images for each phase at 2 s intervals were obtained.

Time-density curves (TDCs) were created from the circular region of interest (ROI) drawn over the SPN, aorta or common carotid artery (if the aorta was not included in the section). The ROI was as large as possible to minimize noise but with care to avoid a partial-volume effect. If there was a substantial artifact from cardiac motion or beam hardening from adjacent bone to create rapid changes of attenuation, or if the proper scan level was not attained due to improper respiration, the image was eliminated from data analysis.

Gamma-variate fits were performed on the time-density curves to remove recirculation of the same data to confirm reproducibility on 2 separate occasions. The gamma variate fit used in this study was expressed by the following equation:

$$C(t)=K(t-At)^{\alpha}e^{-(t-At)/\beta}$$

C(t): represents increasing value of the CT number; t: time after the start of injection; K: constant scale factor; α and β: fitting parameters, and At: appearance time. This technique was performed with DeltaGraph Pro 3 software (Version; 3.0.4).

Pre-contrast density, peak height in density (PH: the maximum value of the TDC. That is defined as total density minus baseline precontrast density) and S/A ratio (the ratio of the peak height of SPN to aorta) were recorded.

Perfusion of the SPN was calculated by applying a nuclear medicine data processing technique to the time-density data. The equation is as follows [5,9]:

$$\text{Perfusion (ml / min / ml)} = \frac{\text{MG of SPNs TDC (HU / min)}}{\text{PH of the aorta TDC (HU)}}$$

Here MG was the maximum gradient of the SPN TDC.

Enhancement patterns of the SPNs were assessed, which were classified as homogeneous enhancement, heterogeneous enhancement, central enhancement,

peripheral enhancement and no enhancement.

Eleven resected specimens of SPN were selected randomly for advanced pathology analyses, which included 4 cases of squamous cell carcinoma, 3 cases of adenocarcinoma, 2 cases of inflammatory nodules and 2 cases of tuberculoma. Immunohistochemical staining was performed on the specimens with the anti-CD31 antibody by using the avidin-biotin-peroxidase-complex technique. The quantity and morphologic characteristic of mirovessels were investigated in at least 10 different areas throughout the lesion (magnification factor, × 100 and × 200).

All values were expressed as a mean ± standard error. The significance of the difference between groups was analyzed by the unpaired t test. $P<0.05$ was considered statistically significant. Statistical analysis of the enhancement patterns between groups was performed by means of the Kruskal-Wallis rank test. All statistical analyses were performed with StatView software (version J4.02, Abacus Concepts, Inc.).

RESULTS

Eighty patients, 50 men and 30 women, ranging in age from 28 to 85 years (mean 66 ± 11.2 SD), with SPNs 5-30 mm (mean 20.15 ± 7.25 SD) in diameter were studied. Final diagnoses were confirmed histologically or cytologically by means of surgery, CT guided transthoracic needle aspiration biopsy and transbronchial lung biopsy in 69 patients. In the remaining 11 patients, diagnoses were based on the clinical data such as whether the nodule showed no radiological evidence of growth in 2 or more years follow-up, or resolution of the lesion on serial chest radiographs after antibiotic treatment. Some patients had a definite diagnoses determined by 1 or more examinations listed above. Of the 80 patients, 52 were diagnosed as malignant, including adenocarcinoma (33 patients), squamous cell carcinoma (11 patients), small cell carcinoma (5 patients), large cell carcinoma (3 patients); 28 were diagnosed as benign, including granuloma or tuberculoma (16 patients) and hamartoma (2 patients). The other 10 benign cases were labeled as active inflammatory nodules, of which 6 were organizing pneumonia, 2 were tuberculosis and 2 were resolved after antibiotic treatment. In analysis we separated active inflammatory nodules from the other benign nodules. In this way patients were divided into 3 groups: malignant group (patients with malignant neoplasm), benign group (patients with granulomas or benign neoplasm), and inflammatory group (patients with active inflammatory nodules).

Malignant, benign and inflammatory nodules showed different appearances in time-density curves. Malignant nodules usually had a moderate increase of the time-density curve as contrast medium appeared in the thoracic aorta, and progressively increased to the peak height, then maintained a plateau. Benign nodules had only a little or no increase after injection of the contrast medium. Conversely, inflammatory nodules showed a rapid increase post-contrast medium injection, the curve reached maximum enhancement then fell and rose again thereafter (Fig.1).

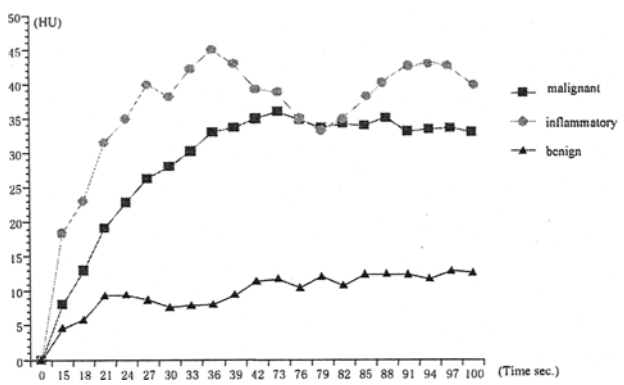

Fig.1. Time-density curves of the malignant, benign and inflammatory nodules.

The precontrast density of the inflammatory nodules was significantly lower than that of the malignant nodules ($P<0.05$, Table 1). The precontrast density of the benign nodules was higher than that of the inflammatory nodules, but not reaching statistical significance.

Both the PH and S/A ratio of the malignant nodules and inflammatory nodules were significantly higher than that of the benign nodules ($P<0.001$; $P<0.001$, Table 1). No statistical difference of either the PH or S/A ratio was found between the malignant and

Table 1.Nodule Characteristics of various groups

Parameter (mean ± SE*)	Malignant (n=52)	Benign (n=18)	Inflammatory (n=10)
PH(HU)	42.72 ± 2.45	13.80 ± 2.25*	45.48 ± 8.73
S/A ratio (%)	15.65 ± 0.95	3.62 ± 0.56*	20.53 ± 4.57
Perfusion(ml/min/ml)	0.78 ± 0.09	0.075 ± 0.014*	1.42 ± 0.13
Precontrast density(HU)	27.10 ± 1.62	29.26 ± 3.93	19.68 ± 2.21**

*Difference between the benign group and malignant group, benign group and inflammatory group were statistically significant (P<0.001, P<0.01).
**Difference between the inflammatory group and malignant group was statistically significant (P<0.05).

inflammatory nodules.

In the analysis of perfusion, both the malignant nodules and inflammatory nodules were significantly higher than the benign nodules (P <0.01, P <0.01, Table 1). However the difference of the perfusion between the malignant nodules and the inflammatory nodules was not significant.

Contrast enhancement patterns of SPNs were extremely complex. Of the malignant nodules, 88% (46/52) showed complete homogeneous enhancement (Fig.2), or heterogeneous with tendency to homogeneous, and 12% (6/52) developed peripheral enhancement owing to central small necrosis (Fig.3). One of the benign nodules showed homogeneous enhancement, 1 nodule appeared as slightly central enhancement, 4 (22%) nodules enhanced in a peripheral or ring-like fashion, and 12 (67%) had no or little enhancement(Fig.4).

Of the inflammatory nodules, 1 showed homogenous enhancement, 3 (30%) nodules showed heterogeneous enhancement (Fig.5) and 6 (60%) developed peripheral enhancement. The peripheral enhancement of inflammatory nodules showed much more irregularity, as compared to the same pattern of some malignant nodules. The differences in the enhancement patterns within the 3 groups were statistically significant (P <0.001).

Pathologic investigation of immunohistochemical staining specimens showed an abundance of immature tumor microvessels in malignant nodules. Inflammatory nodules showed numerous dilated mature capillary vessels, while there were few stained vessels in the tuberculomas (Fig.6).

DISCUSSION

The pharmacokinetics of radiographic contrast media can be approximated in a 2-compartment model with intravascular and extravascular compartments. For the initial period following intravenous injection, contrast enhancement will be largely due to contrast medium within the intravascular space. The delivery of contrast medium to the tissues during the first pass will largely depend on blood flow. As time progresses, contrast medium will pass from the intravascular space into the extravascular space. In this later phase, tissue enhancement will be partly due to intravascular and partly due to extravascular sources. [4-6] Contrast medium kinetics for SPN were somewhat inferred from the SPN time-density curves. The difference in appearance of the time-density curves between the malignant and benign nodules mainly reflected the differences in the volume of extracellular fluid and the diffusing spread of the contrast medium. Lesser contrast material is delivered in hypovascular benign nodules than in malignant nodules, and the diffusion is a slower process in the benign nodules. The immunohistochemical pathologic investigation showed that inflammatory nodules abound with dilated capillary vessels, while malignant nodules were full of mostly immature tumor microvessels. Those findings could explain why inflammatory nodules appeared as a rapid increase in the time-density curve in the early phase, as malignant nodules did. Immature tumor microvessels in malignant tumors are associated with increased blood volume and capillary permeability. Therefore, washout of contrast medium

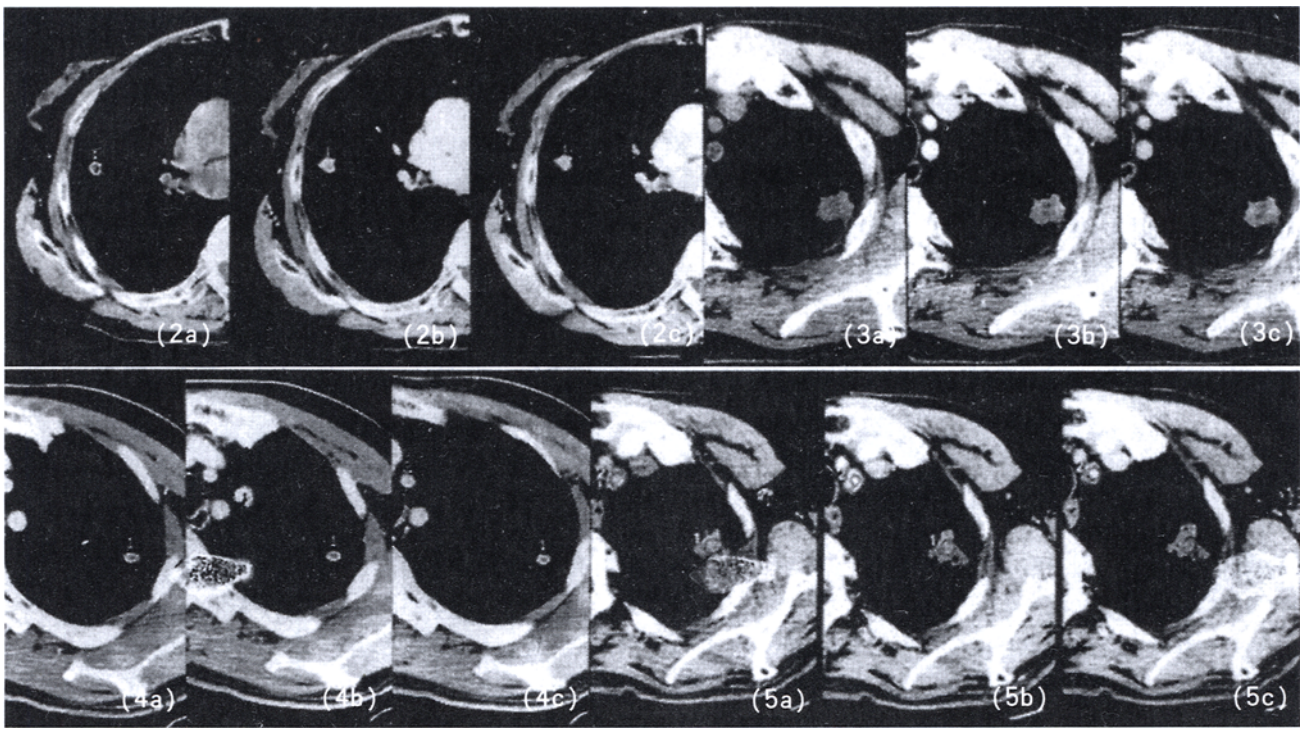

Fig.2. Enhancement pattern of malignant nodule. Patient 61, a 40-year-old man with adenocarcinoma of the right upper lobe. Nodule appeared as homogeneous enhancement. The mean attenuation value was 32.4 HU on the precontrast image (2a), 41.50 HU at 29 s (2b), and 66.60 HU at 100 s (2c) after injection of contrast medium.

Fig.3. Enhancement pattern of malignant nodule. Patient 73, a 63-year-old man with adenocarcinoma of the left upper lobe. Nodule peripheral enhancement owing to central small necrosis. The mean attenuation value was 8 HU on the precontrast image (3a), 26 HU at 24 s (3b), and 36 at 65 s (3c) after injection of contrast medium.

Fig.4. Enhancement pattern of benign nodule. Dynamic CT scans in patient 38, a 45-year-old man with granuloma of the left upper lobe. Nodule showed little enhancement. The mean attenuation value was 28 HU at 15 s (4a), 32 HU at 32 s (4b), and 30 HU at 60 s (4c) after injection of contrast medium.

Fig.5. Enhancement pattern of inflammtary nodule. Dynamic CT scans in patient 57, a 63-year-old man with tuberculosis of the left upper lobe. Nodule showed heterogeneous enhancement. The mean attenuation value was 20 HU at 15 s (5a), 39 HU at 32 s (5b), and 25 HU at 100 s (5c) after injection of contrast medium.

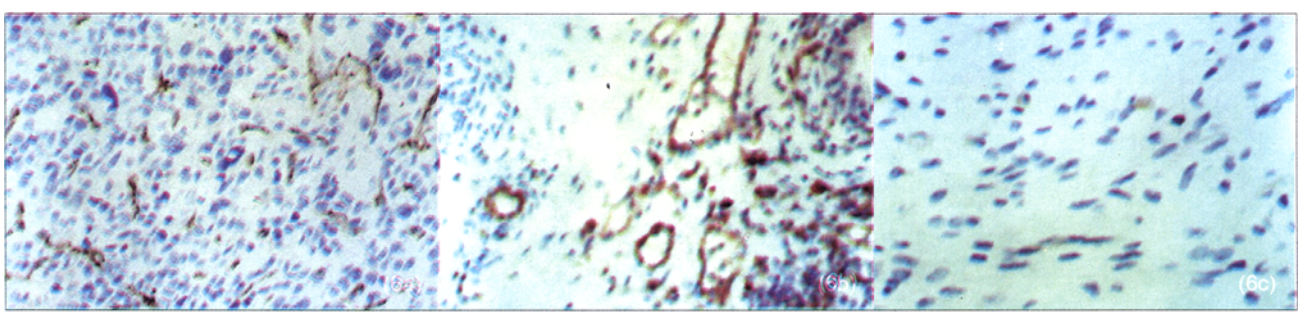

Fig.6. Immunohistochemical staining specimens (× 200) showed abundance of immature tumor microvessels in malignant nodules(6a); Inflammatory nodules appeared with many dilated mature capillary vessels(6b); Few stained vessels in the tuberculoma (6c).

may be less of a consideration for the tumors than for some normal tissues. That may explain why malignant nodules had a prolonged increase of the time-density curve during the late phase. The time-density curve for SPN after contrast medium injection could be based on the distinct differences in the vascularity of benign and malignant nodules. These results are consistent with our previous study with dynamic-contrast enhanced MRI.[12]

This study indicated that the PH might be helpful in distinguishing benign nodules from malignant nodules. Malignant nodules tended to enhance significantly more than benign nodules. These results corroborate the findings of some previous researches. A multicenter study by Swensen, et al. concluded that the absence of significant lung-nodule enhancement on CT is a strong indication of benignity. They studied 356 lung nodules with 15 HU as the threshold, and obtained 98% sensitivity, 58% specificity, and 77% accuracy. [11] If we take 15 HU as a threshold to evaluate the nodules in our study, and if nodules with PH higher than 15 HU were considered malignant, we would receive 96.15% sensitivity, 57.14% specificity and 82.5% accuracy. The positive predictive value would be 76.92, and negative predictive value would be 88.89.

The value of PH, as an absolute measurement of nodule enhancement would be simple and ideal, and could be a semi-quantitative measure of perfusion, but simple measurements of contrast enhancement within tissues are significantly influenced by the effects of inter-patient variations in cardiac output and central vessel blood volume.[9] To minimize the differences in the cardiac output by individuals, we used the S/A ratio by calculating PH of the SPN / PH of the aorta. The data taken in this way offered a more physiologically based measurement than a simple measurement of contrast enhancement. In the analysis of the S/A ratio, no malignant nodule had a S/A ratio less than 6%. If we consider a S/A ratio of 6% as a complementary threshold to evaluate the nodules, there would be no false negatives. There were also no benign nodules with a S/A ratio higher than 6%. This information might be useful clinically.

False positive results were almost due to inflammatory processes in this study. This finding is consistent with other radiological studies. Swensen et al. indicated that younger granulomas with active inflammatory changes generally enhance substantially more than 15 HU. [11] The PH and S/A ratio of the inflammatory nodules were significantly higher than that of the benign nodules, and no significant differences were found as compared with the malignant nodules in our study. Almost all of the active inflammatory nodules would become false positive cases if we evaluate SPNs simply on the basis of the PH or S/A ratio. Abundant dilated capillary vessels invested in inflammatory nodules would contribute to the high enhancement of the inflammatory nodules. In any case, as we discussed above, the type of time-density curve may depict the hemodynamic characteristics of the malignant and inflammatory nodules and may be helpful in differentiation of active inflammatory nodules and malignant nodules. Furthermore, active inflammatory nodules, with less compact tissue structure, appear to have lower density than malignant nodules in plain CT images (P <0.05). They usually have an infiltrative margin with more irregular peripheral enhancement, whereas almost all of the malignant nodules appeared as complete homogenous enhancement or heterogeneous tending to homogenous enhancement. Thus, it would seem that further discrimination between active inflammatory and malignant nodules in patients with a high PH and S/A ratio might be possible by taking into account the precontrast density, enhancement patterns and the appearance of the time-density curve observed on dynamic CT, as well as morphologic features.

Angiogenesis describes a fundamental process in the development of tumors. The development of new vessels within tumors determine their appearance on contrast enhanced CT. Thus, the changes in contrast enhancement that result from tumor angiogenesis can be exploited to provide diagnostic and prognostic information for patients with cancer. [13] Using quantitative analysis and functional imaging to evaluate contrast enhancement of tumors can improve

the radiological assessment of many tumors. Our protocol allows satisfactory measurement of the enhancement of the SPNs and provides quantitative information about tissue perfusion of the malignant, benign and inflammatory pulmonary nodules. As would be expected, measured perfusion was higher in the malignant nodules (0.78 ± 0.09 ml /min /ml) than in the benign nodules (0.075 ± 0.014 ml /min /ml) (P<0.01). The availability of this technique provided physiological correlates for microscopic changes that occur with tumor angiogenesis. This technique is simple, and can be performed with conventional CT. The quantifiable hemodynamic change is considered helpful not only in differential diagnosis, but also in tumor grading, prognosis and therapy monitoring.

The main limitation of the CT technique is that only 1 section level can be readily studied. A technique for the calculation of blood flow through a 3-dimensional reconstruction of the SPNs would have produced a result more representative than that reported.

In summary: dynamic functional CT offers an alternate noninvasive option in the evaluation and management of solitary pulmonary nodules. Lesions demonstrating a high PH or S/A ratio and with high perfusion should be considered as a high possibility of malignancy until proved otherwise. Meanwhile attention should be paid to parameters to eliminate the possibility of an active inflammatory process by investigating precontrast density, enhancement pattern as well as appearance of the time-density curve. More important, lesions with low a PH, S/A ratio and low perfusion were always benign.

REFERENCES

1 Zielinski KW, Kulig A. Morphology of the microvascular bed in primary human carcinomas of lung. Part I. Three-dimensional pattern of microvascular network. Pathol Res Pract. 1984; 178:243–250.

2 Zielinski KW, Kulig A. Morphology of the microvascular bed in primary human carcinomas of lung. II. Mopholometrc investigations of microvascular bed of lung tumors. Pathol Res Pract. 1984; 178:369–377.

3 Blomley MJK, Coulden R, Bufkin C, et al. Contrast bolus dynamic computed tomography for the measurement of solid organ perfusion. Invest Radiol. 1993; 28:s72–s77.

4 Miles KA. Measurement of tissue perfusion by dynamic computed tomography. Br J Radiol. 1991; 64:409–412.

5 Miles KA. Tumour angiogenesis and its relation to contrast enhancement on computed tompgraphy: a review. Eur J Radiol. 1999; 30:198–205.

6 Miles KA, Hayball MP, Dixon AK. Functional imaging of changes intrarenal perfusion using quantitative dynamic computed tomography. Invest Radiol. 1994; 29:911–914.

7 Blomley MJ, Coulden R, Dawson P, et al. Liver perfusion studied with ultrafast CT. J Comput Assist Tomogr. 1995; 19:424–433.

8 Platt JF, Francis IR, Ellis JH, et al. Liver metastases: early detection based on abnormal contrast material enhancement at dual-phase helical CT. Radiology. 1997; 205:49–53

9 Zhang M, Kono M. Solitary pulmonary nodules: Evaluation of blood flow patterns with dynamic CT. Radiology. 1997; 205:471–478.

10 Zhang M, Kono M. Ideal contrast medium bolus for perfusion measurement in dynamic lung CT. Radiology. 1998; 2:583–585.

11 Swensen SJ, Viggiano RW, Midthun DE, et al. Lung nodule enhancement at CT: Multicenter study. Radiology. 2000; 214:73–80.

12 Zhang M, Zou Y, Shang D, et al. Solitary pulmonary nodules: Quantitative investigation with dynamic MR imaging. Chin J Radiol. 2002; 36:592–597.

13 Miles KA. Functional computed tomography in oncology. Eur J Cancer. 2002; 38:2079–2084.